

A multi-D model for Raman amplification

by M. Colin and T. Colin,
Université de Bordeaux

IMB, INRIA Bordeaux Sud Ouest, Team MC2
351 cours de la libération, 33405 Talence cedex, France.

mcolin@math.u-bordeaux1.fr
colin@math.u-bordeaux1.fr

Abstract : In this paper, we continue the study of the Raman amplification in plasmas that we have initiated in [5] and [6]. We point out that the Raman instability gives rise to three components. The first one is colinear to the incident laser pulse and counter propagates. In 2-D, the two other ones make a non-zero angle with the initial pulse and propagates forward. Furthermore they are symmetric with respect to the direction of propagation of the incident pulse. We construct a nonlinear system taking into account all these components and perform some 2-D numerical simulations.

Key words: Zakharov system, Raman amplification, three waves mixing.

1 Introduction

The interaction of powerfull laser pulse with a plasma gives rise to several complex multiscale phenomena. It is of great interest since it occurs in the laboratory simulations of nuclear fusion (NIF, Laser Mega Joule). One of the key mechanism is the Raman instability that can be coupled with Landau damping (see [1]). In [5] and [6], we have initiated a quite systematical mathematical study of the Raman amplification process in plasma by justifying nonlinear models in 1-D and 2-D. These models relies on the propagation of three kind of waves : the initial laser pulse (K_0, ω_0), the Raman component (K_R, ω_R) and the electronic plasma wave ($K_1, \omega_{pe} + \omega_1$) where K and ω stands respectively for the wave vector and the frequency and ω_{pe} is the electronic plasma frequency. In order to be efficient, the interaction has to be a three waves mixing that is the data must satisfy the following relationships :

- The dispersion relation for electromagnetic waves

$$\omega_0^2 = \omega_{pe}^2 + c^2|K_0|^2, \quad (1.1)$$

$$\omega_R^2 = \omega_{pe}^2 + c^2|K_R|^2, \quad (1.2)$$

AMS classification scheme number: 35Q55, 35Q60, 78A60, 74S20

where c is the velocity of light in the vacuum.

- The dispersion relation for electronic plasma waves

$$(\omega_{pe} + \omega_1)^2 = \omega_{pe}^2 + v_{th}^2 |K_0|^2, \quad (1.3)$$

where v_{th} denotes the thermal velocity of the electrons, see below (section 2.1) for its value.

- The three waves resonance conditions

$$\omega_0 = \omega_{pe} + \omega_R + \omega_1, \quad (1.4)$$

$$K_0 = K_R + K_1. \quad (1.5)$$

Even in 2-D, one can find solutions of this system such that K_1 , K_R and K_0 are colinear. This corresponds to the solution used in [5], [6]. The aim of this paper is to provide a more general study in order to understand the influence of the geometry. We solve (1.1) – (1.5) numerically and show that there exists infinitely many solutions in the plane. We compute the amplification rates associated to these solutions and show that the backward solution has a maximum amplification rate when it is colinear to the initial pulse, while the most two amplified forward directions make a non-zero angle with the laser pulse and are symmetric with respect to the direction of propagation of the incident pulse. (see Section 2 and Section 3).

In Section 4, we introduce a nonlinear model taking into account both direction of propagations. First, denote by A_0 the incident laser field, K_0 and ω_0 the associated wave vector and frequency, A_{R_1} the backscattered Raman component K_{R_1} and ω_{R_1} the associated wave vector and frequency, A_{R_2} , the forward Raman component K_{R_2} and ω_{R_2} the associated wave vector and frequency, and finally $A_{R_2^s}$ the second forward Raman component, $K_{R_2^s}$ and $\omega_{R_2^s}$ the associated wave vector and frequency. We assume that K_0 is colinear to the x -axis and then K_{R_2} and $K_{R_2^s}$ are symmetric with respect to the x -axis. $\langle n_e \rangle$ is the low-frequency variation of the density of ions. Furthermore, we put

$$K_0 = \begin{pmatrix} k_0 \\ 0 \end{pmatrix}, \quad K_{R_1} = \begin{pmatrix} k_{R_1} \\ \ell_{R_1} \end{pmatrix}, \quad K_{R_2} = \begin{pmatrix} k_{R_2} \\ \ell_{R_2} \end{pmatrix}, \quad K_{R_2^s} = \begin{pmatrix} k_{R_2^s} \\ \ell_{R_2^s} \end{pmatrix},$$

$$\theta_{1,1} = K_{1,1} \cdot X - \omega_{1,1} t, \quad \theta_{1,2} = K_{1,2} \cdot X - \omega_{1,2} t, \quad \theta_{1,2^s} = K_{1,2^s} \cdot X - \omega_{1,2^s} t.$$

The system reads in a nondimensional form

$$\begin{aligned} i \left(\partial_t + \frac{c^2 k_0^2}{\omega_0^2} \partial_x \right) A_0 + \left(\frac{c^2 k_0^2}{2\omega_0^2} \Delta - \frac{c^4 k_0^4}{2\omega_0^4} \partial_x^2 \right) A_0 &= \frac{\omega_{pe}^2}{2\omega_0^2} \langle n_e \rangle A_0 \quad (1.6) \\ - \nabla \cdot E \left(A_{R_1} e^{-i\theta_{1,1}} \frac{k_{R_1}}{|K_{R_1}|} + \alpha (A_{R_2} e^{-i\theta_{1,2}} + A_{R_2^s} e^{-i\theta_{1,2^s}}) \frac{k_{R_2}}{|K_{R_2}|} \right), \end{aligned}$$

$$\begin{aligned} i \left(\partial_t + \frac{c^2 k_0}{\omega_{R_1} \omega_0} K_{R_1} \cdot \nabla \right) A_{R_1} + \frac{1}{2\omega_{R_1} \omega_0} \left(c^2 k_0^2 \Delta - \frac{c^4 k_0^2}{\omega_{R_1}^2} (K_{R_1} \cdot \nabla)^2 \right) A_{R_1} \\ = \frac{\omega_{pe}^2}{2\omega_0 \omega_{R_1}} \langle n_e \rangle A_{R_1} - \nabla \cdot E^* A_0 e^{i\theta_{1,1}} \frac{k_{R_1}}{|K_{R_1}|}, \quad (1.7) \end{aligned}$$

$$\begin{aligned}
& i \left(\partial_t + \frac{c^2 k_0}{\omega_{R_2} \omega_0} K_{R_2} \cdot \nabla \right) A_{R_2} + \frac{1}{2\omega_{R_2} \omega_0} \left(c^2 k_0^2 \Delta - \frac{c^4 k_0^2}{\omega_{R_2}^2} (K_{R_2} \cdot \nabla)^2 \right) A_{R_2} \\
& = \frac{\omega_{pe}^2}{2\omega_0 \omega_{R_2}} < n_e > A_{R_2} - \alpha \nabla \cdot E^* A_0 e^{i\theta_{1,2}} \frac{k_{R_2}}{|K_{R_2}|}, \tag{1.8}
\end{aligned}$$

$$\begin{aligned}
& i \left(\partial_t + \frac{c^2 k_0}{\omega_{R_2} \omega_0} K_{R_2^s} \cdot \nabla \right) A_{R_2^s} + \frac{1}{2\omega_{R_2} \omega_0} \left(c^2 k_0^2 \Delta - \frac{c^4 k_0^2}{\omega_{R_2}^2} (K_{R_2^s} \cdot \nabla)^2 \right) A_{R_2^s} \\
& = \frac{\omega_{pe}^2}{2\omega_0 \omega_{R_2}} < n_e > A_{R_2^s} - \alpha \nabla \cdot E^* A_0 e^{i\theta_{1,2^s}} \frac{k_{R_2}}{|K_{R_2}|}, \tag{1.9}
\end{aligned}$$

$$\begin{aligned}
i \partial_t E + \frac{v_{th}^2 k_0^2}{2\omega_{pe} \omega_0} \Delta E & = \frac{\omega_{pe}}{2\omega_0} < n_e > E + \nabla \left(A_0 A_{R_1}^* e^{i\theta_{1,1}} \frac{k_{R_1}}{|K_{R_1}|} \right. \\
& \left. + \alpha (A_0 A_{R_2}^* e^{i\theta_{1,2}} + A_0 A_{R_2^s}^* e^{i\theta_{1,2^s}}) \frac{k_{R_2}}{|K_{R_2}|} \right), \tag{1.10}
\end{aligned}$$

$$\begin{aligned}
\left(\partial_t^2 - c_s^2 \Delta \right) < n_e > & = \frac{4m_e}{m_i} \frac{\omega_0 \omega_{R_1}}{\omega_{pe}^2} \Delta \left(|E|^2 + \frac{\omega_{pe}}{\omega_0} |A_0|^2 + \frac{\omega_{pe}}{\omega_{R_1}} |A_{R_1}|^2 \right. \\
& \left. + \frac{\omega_{pe}}{\omega_{R_2}} (|A_{R_2}|^2 + |A_{R_2^s}|^2) \right). \tag{1.11}
\end{aligned}$$

The constants c , c_s , m_e and m_i are respectively the velocity of light in vacuum, the acoustic velocity, the electron's and ion's mass. The methods of [5] applies and one gets the following theorem .

Theorem 1.1. *Let $s > \frac{d}{2} + 3$, $(a_0, a_{R_1}, a_{R_2}, a_{R_2^s}, e) \in (H^{s+2}(\mathbb{R}^d))^5$, $n_0 \in H^{s+1}(\mathbb{R}^d)$ and $n_1 \in H^s(\mathbb{R}^d)$. There exists $T > 0$ and a unique maximal solution $(A_0, A_{R_1}, A_{R_2}, A_{R_2^s}, E, < n_e >)$ to (1.6) – (1.11) such that*

$$\begin{aligned}
(A_0, A_{R_1}, A_{R_2}, A_{R_2^s}, E) & \in \left(C([0, T]; H^{s+2}) \right)^5, \\
< n_e > & \in C([0, T]; H^{s+1}) \cap C^1([0, T]; H^s),
\end{aligned}$$

with initial value

$$\begin{aligned}
(A_0, A_{R_1}, A_{R_2}, A_{R_2^s}, E)(0) & = (a_0, a_{R_1}, a_{R_2}, a_{R_2^s}, e) \\
< n_e > (0) & = n_0, \quad \partial_t < n_e > (0) = n_1.
\end{aligned}$$

In Section 5, we perform some numerical simulations in order to illustrate the phenomena and to emphasize the new directions of propagation.

2 Obtaining a 3-D Raman amplification system

2.1 The Euler-Maxwell system

As noticed in the introduction, the main drawback of the model developped in [5] is the fact that the Raman component and the laser incident field are colinear in the sense that the wave vectors are proportional (in opposite direction). The aim of this section is to get rid of this hypothesis. We will only sketch the computations that are very closed to the ones done in [5]. We start from the bifluid Euler-Maxwell system. The Euler equations are

$$(n_0 + n_e) (\partial_t v_e + v_e \cdot \nabla v_e) = -\frac{\gamma_e T_e}{m_e} \nabla n_e - \frac{e(n_0 + n_e)}{m_e} (E + \frac{1}{c} v_e \times B), \quad (2.1)$$

$$(n_0 + n_i) (\partial_t v_i + v_i \cdot \nabla v_i) = -\frac{\gamma_i T_i}{m_i} \nabla n_i + \frac{e(n_0 + n_i)}{m_i} (E + \frac{1}{c} v_i \times B), \quad (2.2)$$

$$\partial_t n_e + \nabla \cdot ((n_0 + n_e) v_e) = 0, \quad (2.3)$$

$$\partial_t n_i + \nabla \cdot ((n_0 + n_i) v_i) = 0. \quad (2.4)$$

The Maxwell system is written in terms of the electric-magnetic fields for the study of the electronic-plasma waves (Langmuir waves)

$$\partial_t B + c \nabla \times E = 0, \quad (2.5)$$

$$\partial_t E - c \nabla \times B = 4\pi e ((n_0 + n_e) v_e - Z(n_0 + n_i) v_i), \quad (2.6)$$

while the formulation with magnetic potential, electric potential and electric field in the Lorentz jauge is used for the study of the electromagnetic waves (light)

$$\partial_t \psi = c \nabla \cdot A, \quad (2.7)$$

$$\partial_t A + c E = c \nabla \psi, \quad (2.8)$$

$$\partial_t E - c \nabla \times \nabla \times A = 4\pi e ((n_0 + n_e) v_e - Z(n_0 + n_i) v_i), \quad (2.9)$$

where Z is the atomic number of the ions. We first perform a linear analysis of system (2.1) – (2.9) and compute the dispersion relations as well as the polarizations conditions. Then using the time enveloppe approximation, we derive a quasilinear system describing the interaction.

2.2 Dispersion relations and polarization conditions.

Since the mass of the ions is much larger than that of the electrons (a ratio of at least 10^3), the velocity of the ions is smaller than that of the electrons. Therefore we can neglect the contribution of the ions in the current in (2.6) or (2.9). We then linearize System (2.1) – (2.9) around the steady state solution 0

and one gets

$$n_0 \partial_t v_e = -\frac{\gamma_e T_e}{m_e} \nabla n_e - \frac{e n_0}{m_e} E, \quad (2.10)$$

$$\partial_t n_e + n_0 \nabla \cdot v_e = 0, \quad (2.11)$$

$$\partial_t B + c \nabla \times E = 0, \quad (2.12)$$

$$\partial_t E - c \nabla \times B = 4\pi e n_e v_e, \quad (2.13)$$

Note that the acoustic part concerning the ions is decoupled from the high frequency part concerning the electrons and will be considered below. We look for plane wave solutions to (2.10) – (2.11) under the form $e^{i(K \cdot X - \omega t)}(v_e, n_e, B, R)$. Two kind of waves can propagate :

i) Longitudinal waves for which K is parallel to E (electronic-plasma wave). They satisfy the dispersion relation

$$\omega^2 = \omega_{pe}^2 + v_{th}^2 |K|^2, \quad (2.14)$$

with

$$\omega_{pe}^2 = \frac{4\pi e^2 n_0}{m_e}, \quad v_{th}^2 = \sqrt{\frac{\gamma_e T_e}{m_e}}.$$

ii) Transverse waves for which K is orthogonal to E (electromagnetic waves). They obey the dispersion relation

$$\omega^2 = \omega_{pe}^2 + c^2 |K|^2. \quad (2.15)$$

Since for our applications, $v_{th} \ll c$, the shape of the graph of (2.14) or (2.15) are very different. Indeed, (2.14) is very flat near the origin compare to (2.15) (see Figure 1).

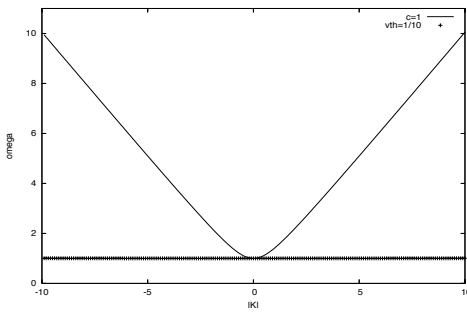


Figure 1: Plot of the first part of the dispersion relations (2.14) (dashed line) and (2.15) (solid line) with $\omega_{pe}^2 = 1$, $c^2 = 1$ and $v_{th}^2 = 0.01$. The plot corresponds to ω as a function of $|K|$.

Therefore, even if a precise couple (K_0, ω_0) is imposed for the incident laser field, we have to consider only the frequency ω_{pe} for the electronic plasma wave with a continuous range K of wave vectors. Therefore, the complete solution reads

$$\begin{pmatrix} B \\ E \\ v_e \\ n \end{pmatrix} = \begin{pmatrix} B_{||} \\ E_{||} \\ v_{e||} \\ n_e \end{pmatrix} e^{-i\omega_{pe}t} + \sum_{j=1}^n \begin{pmatrix} B_{\perp}^j \\ E_{\perp}^j \\ v_{e\perp}^j \\ 0 \end{pmatrix} e^{i(K_j \cdot X - \omega_j t)} + c.c. \quad (2.16)$$

where $||$ corresponds to the longitudinal part and \perp corresponds to the transverse part. Furthermore, for all $1 \leq j \leq n$

$$\omega_j^2 = \omega_{pe}^2 + c^2 |K_j|^2. \quad (2.17)$$

As usual $(B_{||}, E_{||}, v_{e||}, n_e)$ and $(B_{\perp}^j, E_{\perp}^j, v_{e\perp}^j)$ satisfy some polarization conditions that are obtained like in [5] by plugging plane waves in (2.10) – (2.13).

$$v_{e||} = -i \frac{i\omega_{pe}}{4\pi e n_0} E_{||}, \quad B_{||} = 0, \quad n_e = -\frac{1}{4\pi e} \nabla \cdot E_{||}.$$

For the transverse part, one writes $B_{\perp} = \nabla \times A_{\perp}$ and using the Maxwell system in the Lorentz gauge we get

$$-i\omega_j A_{\perp}^j + c E_{\perp}^j = 0, \quad (2.18)$$

$$-i\omega_j E_{\perp}^j + c K_j \times K_j \times A_{\perp}^j = 4\pi n_0 v_{e\perp}, \quad (2.19)$$

$$-i\omega_j v_{e\perp}^j = -\frac{e}{n_e} E_{\perp}^j. \quad (2.20)$$

Using (2.19) and (2.20), one obtains

$$-i\omega_j E_{\perp}^j + c K_j \times K_j \times A_{\perp}^j = -i \frac{4\pi e^2 n_0}{m_e \omega_j} E_{\perp}^j.$$

It follows that E_{\perp}^j is orthogonal to K_j and therefore so do A_{\perp}^j and $v_{e\perp}^j$. In a 2-D geometry, this leads to look for E_{\perp}^j , A_{\perp}^j and $v_{e\perp}^j$ under the form

$$(E_{\perp}^j, A_{\perp}^j, v_{e\perp}^j) \frac{K_j^{\perp}}{|K_j|}, \quad (2.21)$$

where $(E_{\perp}^j, A_{\perp}^j, v_{e\perp}^j)$ denote now scalar functions. The polarization relations on these scalar fields read

$$v_{e\perp}^j = \frac{e}{m_e c} A_{\perp}^j, \quad E_{\perp}^j = i \frac{\omega_j}{c} A_{\perp}^j. \quad (2.22)$$

2.3 The weakly nonlinear theory.

We restrict ourself to the 2D case. Since we are interested in the Raman instability, we take $n = 2$ in (2.16) write

$$\begin{pmatrix} B \\ E \\ v_e \\ n \end{pmatrix} = \begin{pmatrix} 0 \\ E_{||} \\ v_{e||} \\ n_e \end{pmatrix} e^{-i\omega_{pe}t} + \begin{pmatrix} B_0 \\ E_0 \\ v_{e0} \\ 0 \end{pmatrix} e^{i(K_0 \cdot X - \omega_0 t)} \\ + \begin{pmatrix} B_R \\ E_R \\ v_{eR} \\ 0 \end{pmatrix} e^{i(K_R \cdot X - \omega_R t)} + c.c., \quad (2.23)$$

where 0 stands for the incident laser field and R for the Raman component. The equations satisfied by each of the electromagnetic fields (B_0, E_0, v_{e0}) and (B_R, E_R, v_{eR}) are, using the vector potential A ($A = A_0$ or A_R)

$$\partial_t^2 A + c^2 \nabla \times \nabla \times A = -4\pi e c (n_0 + n_e) v_e.$$

The polarization condition (2.21) leads to

$$\partial_t^2 A - c^2 \Delta A = -4\pi e c \mathbf{P}_{K^\perp} ((n_0 + n_e) v_e),$$

where \mathbf{P}_{K^\perp} is the orthogonal projector onto K^\perp . Now we write

$$A = \tilde{A} e^{i(K \cdot X - \omega t)} + c.c.$$

(with $K = K_0$ or K_R , $\omega = \omega_0$ or ω_R) and get

$$\begin{aligned} \partial_t^2 A &= (\partial_t^2 \tilde{A} - 2i\omega \partial_t \tilde{A} - \omega^2 \tilde{A}) e^{i\theta}, \\ \nabla A &= (\nabla \tilde{A} + iK \tilde{A}) e^{i\theta}, \\ \Delta A &= (\Delta \tilde{A} + 2iK \cdot \nabla \tilde{A} - K^2 \tilde{A}) e^{i\theta}, \end{aligned}$$

where $\theta = K \cdot X - \omega t$. At the first order

$$-2i\omega \partial_t \tilde{A} - 2ic^2 K \cdot \nabla \tilde{A} = 0.$$

Therefore

$$\partial_t^2 \tilde{A} = \frac{c^4}{\omega^2} (K \cdot \nabla)^2 \tilde{A}.$$

This is the method used to derive the BBM equation in the water wave theory (see [2] or [4]). We obtain (omitting the tildes)

$$\begin{aligned} &-2i\omega \partial_t A - 2ic^2 K \cdot \nabla A - c^2 \Delta A + \frac{c^4}{\omega^2} (K \cdot \nabla)^2 A + (c^2 K^2 - \omega^2) A \\ &= -4\pi e c \mathbf{P}_{K^\perp} ((n_0 + n_e) v_e) e^{-i\theta}. \end{aligned} \quad (2.24)$$

We now consider a three waves mixing. In a 2-D framework we consider three waves vectors (K_0, K_R, K_1) and three frequencies $(\omega_0, \omega_R, \omega_1)$ satisfying

$$\begin{cases} K_0 = K_R + K_1 \\ \omega_0 = \omega_{pe} + \omega_R + \omega_1 \end{cases},$$

$$K_0 = \begin{pmatrix} k_0 \\ 0 \end{pmatrix}, \quad K_R = \begin{pmatrix} k_R \\ l_R \end{pmatrix}, \quad K_1 = \begin{pmatrix} k_1 \\ l_1 \end{pmatrix}. \quad (2.25)$$

Without loss of generality we assume that the incident laser field propagates along the x -axis. In the right-hand-side of (2.24), the nonlinear term gives using (2.22)

$$(n_0 + n_e)v_e = n_0v_e + n_ev_e = \frac{n_0e}{m_e c}A + n_ev_e.$$

Equation (2.24) then reads

$$\begin{aligned} & -2i\omega\partial_tA - 2ic^2K \cdot \nabla A - c^2\Delta A + \frac{c^4}{\omega^2}(K \cdot \nabla)^2 A + (c^2K^2 - \omega^2)A \\ & = -\omega_{pe}A - 4\pi ec \mathbf{P}_{K^\perp}(n_ev_e)e^{-i\theta}, \end{aligned}$$

and we get

$$i\left(\partial_t + \frac{c^2}{\omega}K \cdot \nabla\right)A + \frac{1}{2\omega}\left(c^2\Delta - \frac{c^4}{\omega^2}(K \cdot \nabla)^2\right)A = \frac{2\pi ec}{\omega} \mathbf{P}_{K^\perp}(n_ev_e)e^{-i\theta}. \quad (2.26)$$

At this step, we have to compute the right-hand-side of (2.26)

$$n_ev_e = \left(\langle n_e \rangle + n_{e||}e^{-i\omega_{pe}t} + c.c. \right) \left(v_{e||}e^{-i\omega_{pe}t} + v_{e0}e^{i\theta_0} \frac{K_0^\perp}{|K_0|} + v_{eR}e^{i\theta_R} \frac{K_R^\perp}{|K_R|} + c.c. \right),$$

where $\langle n_e \rangle$ denotes the low frequency part of the variation of density of ions. We have to use the interaction condition (2.25).

• Equation on A_0 . We keep only the resonant terms in the right-hand-side of (2.26), that is

$$\frac{2\pi ec}{\omega_0} \mathbf{P}_{K^\perp} \left(\langle n_e \rangle v_{e0} \frac{K_0^\perp}{|K_0|} + n_{e||}v_{eR} \frac{K_R^\perp}{|K_R|} e^{-i\theta_1} \right)$$

with

$$n_{e||} = -\frac{1}{4\pi e} \nabla \cdot E_{||}, \quad v_{e0} = \frac{e}{m_e c} A_0, \quad v_{eR} = \frac{e}{m_e c} A_R.$$

Therefore

$$\begin{aligned} & i\left(\partial_t + \frac{c^2}{\omega_0}K_0 \cdot \nabla\right)A_0 + \frac{1}{2\omega_0}\left(c^2\Delta - \frac{c^4}{\omega_0^2}(K_0 \cdot \nabla)^2\right)A_0 \\ & = \frac{2\pi e^2}{\omega_0 m_e} \langle n_e \rangle A_0 - \frac{e}{2\omega_0 m_e} \nabla \cdot E A_R \mathbf{P}_{K_0^\perp} \left(\frac{K_R^\perp}{|K_R|} \right) e^{-i\theta_1}. \end{aligned}$$

Moreover, for any vector a

$$\mathbf{P}_{K_0^\perp}(a) = \frac{K_0^\perp \cdot a}{|K_0^\perp|} \frac{K_0^\perp}{|K_0|}.$$

The 2-D equation for A_0 then reads

$$\begin{aligned} & i \left(\partial_t + \frac{c^2}{\omega_0} K_0 \cdot \nabla \right) A_0 + \frac{1}{2\omega_0} \left(c^2 \Delta - \frac{c^4}{\omega_0^2} (K_0 \cdot \nabla)^2 \right) A_0 \\ &= \frac{2\pi e^2}{\omega_0 m_e} \langle n_e \rangle A_0 - \frac{e}{2\omega_0 m_e} (\nabla \cdot E) A_R e^{-i\theta_1} \frac{K_0 \cdot K_R}{|K_0||K_R|}. \end{aligned} \quad (2.27)$$

- Equation on A_R . A similar computation for A_R gives

$$\begin{aligned} & i \left(\partial_t + \frac{c^2}{\omega_R} K_R \cdot \nabla \right) A_R + \frac{1}{2\omega_R} \left(c^2 \Delta - \frac{c^4}{\omega_R^2} (K_R \cdot \nabla)^2 \right) A_R \\ &= \frac{2\pi e^2}{\omega_R m_e} \langle n_e \rangle A_R - \frac{e}{2\omega_R m_e} (\nabla \cdot E^*) A_0 e^{i\theta_1} \frac{K_0 \cdot K_R}{|K_0||K_R|}. \end{aligned} \quad (2.28)$$

• Equation on E . The electronic-plasma part is very similar to that of [5]. We describe briefly the procedure. Using (2.1), (2.2) and (2.6), one has

$$\begin{aligned} \partial_t^2 E + c^2 \nabla \times \nabla \times E &= 4\pi e \partial_t \left((n_0 + n_e) v_e \right) \\ &= 4\pi (n_0 + n_e) \partial_t v_e + v_e \partial_t n_e \\ &= 4\pi e \left(- (n_0 + n_e) v_e \cdot \nabla v_e - \frac{\gamma_e T_e}{m_e} \nabla n_e \right. \\ &\quad \left. - \frac{e(n_0 + n_e)}{m_e} \left(E + \frac{1}{c} v_e \times B \right) \right) - v_e \nabla \cdot \left((n_0 + n_e) v_e \right). \end{aligned}$$

Keeping only at most quadratic terms gives

$$\begin{aligned} \partial_t^2 E + c^2 \nabla \times \nabla \times E &= 4\pi e \left(- n_0 v_e \cdot \nabla v_e - \frac{\gamma_e T_e}{m_e} \nabla n_e \right. \\ &\quad \left. - \frac{e(n_0 + n_e)}{m_e} E - \frac{e n_0}{c m_e} v_e \times B - n_0 v_e \nabla \cdot v_e \right). \end{aligned}$$

Writting $E = E_{||} e^{-i\omega_{pe} t} + c.c.$ gives

$$\begin{aligned} \partial_t^2 E_{||} + c^2 \nabla \times \nabla \times E_{||} + \omega_{pe}^2 E_{||} &+ \frac{4\pi e \gamma_e T_e}{m_e} \nabla n_e \\ &= 4\pi e \left(- n_0 v_e \cdot \nabla v_e - \frac{e(n_0 + n_e)}{m_e} E_{||} - \frac{e n_0}{c m_e} v_e \times -n_0 v_e \nabla \cdot v_e \right) e^{i\omega_{pe} t}. \end{aligned}$$

Using the polarization condition

$$n_e = -\frac{1}{4\pi e} \nabla \cdot E_{||},$$

we obtain

$$\begin{aligned} & \partial_t^2 E_{||} + c^2 \nabla \times \nabla \times E_{||} - v_{th}^2 \nabla \nabla \cdot E_{||} + \omega_{pe}^2 E_{||} \\ &= 4\pi e \left(-n_0 v_e \cdot \nabla v_e - \frac{e(n_0 + n_e)}{m_e} E_{||} - \frac{en_0}{cm_e} v_e \times -n_0 v_e \nabla \cdot v_e \right) e^{i\omega_{pe} t}. \end{aligned}$$

The nonlinear resonant terms are given by

$$\begin{aligned} v_e \cdot \nabla v_e &= v_0 \cdot \nabla v_R^* + v_R^* \cdot \nabla v_0, \\ n_e E_{||} &= \langle n_e \rangle E_0, \\ v_e \times B &= v_0 \times B_R^* + v_R^* \times B_0, \\ v_e \nabla \cdot v_e &= v_0 \nabla \cdot v_R^* + v_R^* \nabla \cdot v_0, \end{aligned}$$

since v_0 and v_R^* are orthogonal. But

$$B_0 = \nabla \times A_0, \quad v_0 = \frac{e}{m_e c} A_0,$$

then

$$\begin{aligned} -n_e v_e \cdot \nabla v_e - \frac{en_0}{cm_e} v_e \times B &= -\frac{e^2 n_0}{m_e^2 c^2} \left(A_0 \cdot \nabla A_R^* + A_R^* \cdot \nabla A_0 \right. \\ &\quad \left. + A_0 \times \nabla \times A_R^* + A_R^* \times \nabla \times A_0 \right) \\ &= -\frac{e^2 n_0}{m_e^2 c^2} \nabla (A_0 \cdot A_R^*). \end{aligned}$$

Since

$$A_0 \cdot A_R^* = A_0 A_R^* \frac{K_0 K_R}{|K_0||K_R|},$$

it follows that

$$\begin{aligned} & -2i\omega_{pe} \partial_t E_{||} + c^2 \nabla \times \nabla \times E_{||} - v_{th}^2 \nabla \nabla \cdot E_{||} \\ &= -\frac{4\pi e^2 n_0}{m_e} \langle n_e \rangle E_{||} - \frac{4\pi e^3 n_0}{m_e^2 c^2} \nabla (A_0 A_R^* e^{i\theta_1} \frac{K_0 K_R}{|K_0||K_R|}). \end{aligned}$$

The final equation reads denoting $E_0 = E_{||}$

$$\begin{aligned} & i \partial_t E_0 + \frac{v_{th}^2}{2\omega_{pe}} \nabla \nabla \cdot E_0 - \frac{c^2}{2\omega_{pe}} \nabla \times \nabla \times E_0 \\ &= \frac{\omega_{pe}}{2} \langle n_e \rangle E_0 + \frac{e\omega_{pe}}{2m_e c^2} \nabla (A_0 A_R^* e^{i\theta_1} \frac{K_0 \cdot K_R}{|K_0||K_R|}). \end{aligned} \quad (2.29)$$

- Equation on $\langle n_e \rangle$. The acoustic part is the same as in [5] and reads

$$\left(\partial_t^2 - c_s^2 \Delta \right) \langle n_e \rangle = \frac{1}{4\pi n_i} \Delta \left(|E_0|^2 + \frac{\omega_{pe}^2}{c^2} (|A_0|^2 + |A_R|^2) \right), \quad (2.30)$$

where

$$c_s^2 = \frac{\gamma_i T_i}{m_i} + \frac{\gamma_e T_e}{m_e}.$$

System (2.27) – (2.30) is the 2-D Raman interaction system.

3 The amplification rates and the most amplified directions.

3.1 Semi-classical asymptotic.

As in [6], we write a semi-classical limit of System (2.27) – (2.30) in order to obtain amplification rates. Denoting $E_0 = \mathcal{E}e^{i(K_1 \cdot X - \omega_1 t)}$ and writting

$$\partial_t E_0 \ll \omega_1 E_0, \quad \nabla E_0 \ll K_1 E_0$$

leads to

$$i\left(\partial_t + \frac{c^2}{\omega_0} K_0 \cdot \nabla\right) A_0 = \frac{2\pi e^2}{\omega_0 m_e} \langle n_e \rangle A_0 - i \frac{e}{2\omega_0 m_e} K_1 \cdot \mathcal{E} A_R \frac{K_0 \cdot K_R}{|K_0||K_R|}, \quad (3.1)$$

$$i\left(\partial_t + \frac{c^2}{\omega_R} K_R \cdot \nabla\right) A_R = \frac{2\pi e^2}{\omega_R m_e} \langle n_e \rangle A_R - i \frac{e}{2\omega_R m_e} K_1 \cdot \mathcal{E}^* A_0 \frac{K_0 \cdot K_R}{|K_0||K_R|}, \quad (3.2)$$

$$\begin{aligned} i\left(\partial_t - \frac{v_{th}^2}{\omega_{pe}} (K_1 \cdot \nabla)\right) \mathcal{E} + \omega_1 \mathcal{E} - \frac{c^2}{2\omega_{pe}} K_1 \times K_1 \times \mathcal{E} \\ = \frac{\omega_{pe}}{2} \langle n_e \rangle \mathcal{E} + i \frac{\omega_{pe} e}{2m_e c^2} A_0 A_R^* \frac{K_0 \cdot K_R}{|K_0||K_R|} K_1. \end{aligned} \quad (3.3)$$

Now recall that the third wave $(\omega_{pe} + \omega_1, K_1)$ satisfies the dispersion relation (2.14)

$$(\omega_{pe} + \omega_1)^2 = \omega_{pe}^2 + v_{th}^2 |K_1|^2,$$

and thus a direct expansion gives

$$\omega_1 \approx \frac{v_{th}^2 |K_1|^2}{2\omega_{pe}}.$$

Then the equation on \mathcal{E} reads

$$i\left(\partial_t - i \frac{v_{th}^2}{\omega_{pe}} K_1 \cdot \nabla\right) \frac{K_1 \cdot \mathcal{E}}{|K_1|} = \frac{\omega_{pe}}{2} \frac{K_1 \cdot \mathcal{E}}{|K_1|} + i \frac{\omega_{pe} e}{2m_e c^2} A_0 A_R^* \frac{K_0 \cdot K_R}{|K_0||K_R|} |K_1|.$$

Finally, denoting by

$$f_0 = \frac{\omega_{pe}}{c} A_0, \quad f_R = \frac{\omega_{pe}}{c} A_R, \quad f = \frac{K_1 \cdot \mathcal{E}}{|K_1|},$$

Equations (3.1), (3.2) and (3.3) become

$$i\left(\partial_t + \frac{c^2}{\omega_0} K_0 \cdot \nabla\right) f_0 = \frac{2\pi e^2}{\omega_0 m_e} \langle n_e \rangle f_0 - i \frac{e|K_1|}{2\omega_0 m_e} f f_R \cos(\theta), \quad (3.4)$$

$$i\left(\partial_t + \frac{c^2}{\omega_R} K_R \cdot \nabla\right) f_R = \frac{2\pi e^2}{\omega_R m_e} \langle n_e \rangle f_R - i \frac{e|K_1|}{2\omega_R m_e} f^* f_0 \cos(\theta), \quad (3.5)$$

$$i\left(\partial_t - i \frac{v_{th}^2}{\omega_{pe}} K_1 \cdot \nabla\right) f = \frac{\omega_{pe}}{2} \langle n_e \rangle f + i \frac{e|K_1|}{2m_e \omega_{pe}} f_0 f_R^* \cos(\theta), \quad (3.6)$$

where θ denotes the angle between K_0 and K_R .

3.2 Amplification rates.

Let us now consider that f_0 is fixed (it is a pump wave). System (3.5) – (3.6) becomes

$$\partial_t f_R = \frac{e|K_1|}{2m_e\omega_R} f^* f_0 \cos(\theta), \quad (3.7)$$

$$\partial_t f = \frac{e|K_1|}{2m_e\omega_R} f_0 f_R^* \cos(\theta). \quad (3.8)$$

The amplification rate is therefore proportional to

$$\beta = \frac{|K_1|}{\sqrt{\omega_R \omega_{pe}}} |\cos(\theta)|.$$

Recall that the incident field propagates along the x -axis and that

$$K_0 = \begin{pmatrix} k_0 \\ 0 \end{pmatrix}, \quad K_R = \begin{pmatrix} k_R \\ \ell_R \end{pmatrix}, \quad K_1 = \begin{pmatrix} k_1 \\ \ell_1 \end{pmatrix}.$$

Remark that we have $\ell_R = -\ell_1$. The dispersion relation (2.14) and (2.15) gives

$$\begin{cases} \omega_0^2 = \omega_{pe}^2 + k_0^2 c^2, \\ \omega_R^2 = \omega_{pe}^2 + (k_R^2 + \ell_R^2) c^2, \\ (\omega_{pe} + \omega_1)^2 = \omega_{pe}^2 + v_{th}^2 (k_1^2 + \ell_1^2). \end{cases} \quad (3.9)$$

We take ω_{pe} as unit for ω and $\frac{c}{\omega_{pe}}$ as unit for k . Introduce

$$\alpha = \frac{v_{th}}{c} \ll 1,$$

then System (3.9) can be rewritten into

$$\begin{cases} \omega_0^2 = 1 + k_0^2, \\ \omega_R^2 = 1 + (k_R^2 + \ell_R^2), \\ (1 + \omega_1)^2 = 1 + \alpha^2 (k_1^2 + \ell_1^2). \end{cases} \quad (3.10)$$

The amplification rate β is given by

$$\beta = \frac{\sqrt{k_1^2 + \ell_1^2}}{\sqrt{1 + k_R^2 + \ell_1^2}} \frac{|k_R|}{\sqrt{k_R^2 + \ell_1^2}}. \quad (3.11)$$

For given k_0, ω_0 satisfying $\omega_0^2 = 1 + k_0^2$, we therefore need to find the maximum of $\beta(k_R, k_1, \ell_1)$ subject to the constraints

$$\omega_R^2 = 1 + (k_R^2 + \ell_R^2), \quad (1 + \omega_1)^2 = 1 + \alpha^2 (k_1^2 + \ell_1^2), \quad k_0 = k_R + k_1.$$

Replacing k_R by $k_0 - k_1$ in (3.11) gives

$$\beta = \frac{\sqrt{k_1^2 + \ell_1^2}}{\sqrt{1 + (k_0 - k_1)^2 + \ell_1^2}} \frac{|k_0 - k_1|}{\sqrt{(k_0 - k_1)^2 + \ell_1^2}}, \quad (3.12)$$

with

$$\sqrt{1 + k_0^2} = \sqrt{1 + (k_0 - k_1)^2 + \ell_1^2} + \sqrt{1 + \alpha^2 (k_1^2 + \ell_1^2)}. \quad (3.13)$$

3.3 Conclusions.

The above problem (3.12) – (3.13) is solved numerically. The conclusions are the following ones. For the backscattered component ($k < 0$), the maximum is reached for $\ell_1 = 0$. This means that the most amplified direction corresponds to the case where the Raman field is colinear to the incident laser field (see Figure 2).

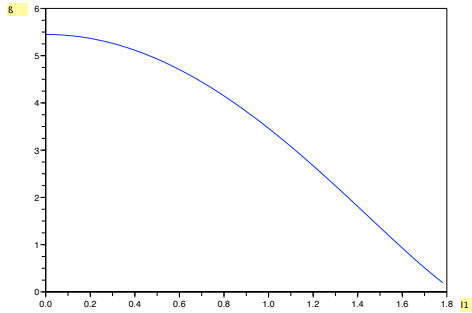


Figure 2: β with respect to ℓ_1 with $k < 0$

This model is used in [5]. For the forward component ($k > 0$), one can see in Figure 3 that the maximum of β is reached for $\ell_1 \neq 0$. Therefore, the Raman field makes a non-zero angle with the incident laser pulse and gives rise to new direction of propagation. It would be a cone in 3-D.

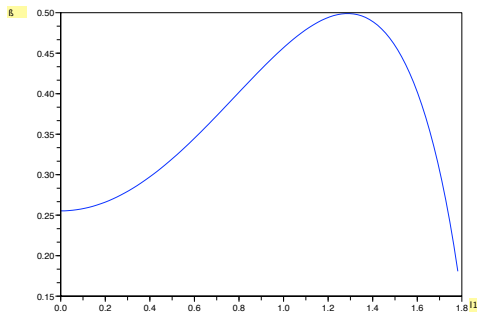


Figure 3: β with respect to ℓ_1 with $k > 0$

The next step is to take into account this new direction.

4 A complete model

4.1 Some basic tools

In order to describe the directions of propagation, one introduces the three wave vectors for the Raman component given by problem (3.12) – (3.13)

$$K_{R_1} = \begin{pmatrix} k_{R_1} \\ \ell_{R_1} \end{pmatrix}, \quad K_{R_2} = \begin{pmatrix} k_{R_2} \\ \ell_{R_2} \end{pmatrix}, \quad K_{R_2^s} = \begin{pmatrix} k_{R_2^s} \\ \ell_{R_2^s} \end{pmatrix},$$

satisfying

$$K_0 = K_{R_1} + K_{1,1} = K_{R_2} + K_{1,2} = K_{R_2^s} + K_{1,2^s},$$

that is

$$\begin{aligned} \begin{pmatrix} k_0 \\ 0 \end{pmatrix} &= \begin{pmatrix} k_{R_1} \\ \ell_{R_1} \end{pmatrix} + \begin{pmatrix} k_{1,1} \\ \ell_{1,1} \end{pmatrix}, \\ &= \begin{pmatrix} k_{R_2} \\ \ell_{R_2} \end{pmatrix} + \begin{pmatrix} k_{1,2} \\ \ell_{1,2} \end{pmatrix}, \\ &= \begin{pmatrix} k_{R_2^s} \\ \ell_{R_2^s} \end{pmatrix} + \begin{pmatrix} k_{1,2^s} \\ \ell_{1,2^s} \end{pmatrix}. \end{aligned}$$

We then introduce the Raman frequencies ω_{R_1} , ω_{R_2} and $\omega_{R_2^s}$ solution to

$$\begin{aligned} \omega_0 &= \omega_{pe} + \omega_{R_1} + \omega_{1,1}, \\ &= \omega_{pe} + \omega_{R_2} + \omega_{1,2}, \\ &= \omega_{pe} + \omega_{R_2^s} + \omega_{1,2^s}. \end{aligned}$$

Note that (K_0, ω_0) , (K_{R_1}, ω_{R_1}) , (K_{R_2}, ω_{R_2}) and $(K_{R_2^s}, \omega_{R_2^s})$ satisfy the dispersion relation for electromagnetic waves (2.15) while $(K_{1,1}, \omega_{1,1})$, $(K_{1,2}, \omega_{1,2})$ and $(K_{1,2^s}, \omega_{1,2^s})$ satisfy the one for electronic-plasma waves (2.14). That means that we have

$$\begin{aligned} \omega_{R_1} &= \sqrt{\omega_{pe}^2 + c^2(k_{R_1}^2 + \ell_{R_1}^2)}, \\ \omega_{R_2} &= \sqrt{\omega_{pe}^2 + c^2(k_{R_2}^2 + \ell_{R_2}^2)}, \\ \omega_{R_2^s} &= \sqrt{\omega_{pe}^2 + c^2(k_{R_2^s}^2 + \ell_{R_2^s}^2)}. \end{aligned}$$

Since K_2 and K_2^s are symmetric with respect to K_0 , choosing K_0 colinear to the x -axis, we have $k_{R_2} = k_{R_2^s}$ and $\ell_{R_2} = -\ell_{R_2^s}$. Therefore, one has $\omega_{R_2} = \omega_{R_2^s}$ and $\omega_{1,2} = \omega_{1,2^s}$. In the sequel, we replace $\omega_{R_2^s}$ and $\omega_{1,2^s}$ by ω_{R_2} and $\omega_{1,2}$.

4.2 The equations.

As in Section 2, one gets the following set of equations, assuming that K_0 is colinear to the x -axis,

$$i\left(\partial_t + \frac{c^2}{\omega_0^2} K_0 \cdot \nabla\right) A_0 + \left(\frac{c^2 k_0^2}{2\omega_0^2} \Delta - \frac{c^4}{2\omega_0^4} (K_0 \cdot \nabla)^2\right) A_0 = \frac{2\pi e^2}{m_e \omega_0} < n_e > A_0$$

$$- \frac{e}{2m_e \omega_0} \nabla \cdot E \left(A_{R_1} e^{-i\theta_{1,1}} \frac{K_0 \cdot K_{R_1}}{|K_0||K_{R_1}|} + A_{R_2} e^{-i\theta_{1,2}} \frac{K_0 \cdot K_{R_2}}{|K_0||K_{R_2}|} + A_{R_2^s} e^{-i\theta_{1,2s}} \frac{K_0 \cdot K_{R_2^s}}{|K_0||K_{R_2^s}|} \right), \quad (4.1)$$

$$i\left(\partial_t + \frac{c^2}{\omega_{R_1}} K_{R_1} \cdot \nabla\right) A_{R_1} + \frac{1}{2\omega_{R_1}} \left(c^2 \Delta - \frac{c^4}{\omega_{R_1}^2} (K_{R_1} \cdot \nabla)^2 \right) A_{R_1}$$

$$= \frac{2\pi e^2}{m_e \omega_{R_1}} < n_e > A_{R_1} - \frac{e}{2m_e \omega_{R_1}} \nabla \cdot E^* A_0 e^{i\theta_{1,1}} \frac{K_0 \cdot K_{R_1}}{|K_0||K_{R_1}|}, \quad (4.2)$$

$$i\left(\partial_t + \frac{c^2}{\omega_{R_2}} K_{R_2} \cdot \nabla\right) A_{R_2} + \frac{1}{2\omega_{R_2}} \left(c^2 \Delta - \frac{c^4}{\omega_{R_2}^2} (K_{R_2} \cdot \nabla)^2 \right) A_{R_2}$$

$$= \frac{2\pi e^2}{m_e \omega_{R_2}} < n_e > A_{R_2} - \frac{e}{2m_e \omega_{R_2}} \nabla \cdot E^* A_0 e^{i\theta_{1,2}} \frac{K_0 \cdot K_{R_2}}{|K_0||K_{R_2}|}, \quad (4.3)$$

$$i\left(\partial_t + \frac{c^2}{\omega_{R_2^s}} K_{R_2^s} \cdot \nabla\right) A_{R_2^s} + \frac{1}{2\omega_{R_2^s}} \left(c^2 \Delta - \frac{c^4}{\omega_{R_2^s}^2} (K_{R_2^s} \cdot \nabla)^2 \right) A_{R_2^s}$$

$$= \frac{2\pi e^2}{m_e \omega_{R_2^s}} < n_e > A_{R_2^s} - \frac{e}{2m_e \omega_{R_2^s}} \nabla \cdot E^* A_0 e^{i\theta_{1,2s}} \frac{K_0 \cdot K_{R_2^s}}{|K_0||K_{R_2^s}|}, \quad (4.4)$$

$$i\partial_t E + \frac{v_{th}^2}{2\omega_{pe}} \Delta E = \frac{\omega_{pe}^2}{2} < n_e > E + \frac{\omega_{pe} e}{2m_e c^2} \nabla \left(A_0 A_{R_1}^* e^{i\theta_{1,1}} \frac{K_0 \cdot K_{R_1}}{|K_0||K_{R_1}|} \right.$$

$$\left. + A_0 A_{R_2}^* e^{i\theta_{1,2}} \frac{K_0 \cdot K_{R_2}}{|K_0||K_{R_2}|} + A_0 A_{R_2^s}^* e^{i\theta_{1,2s}} \frac{K_0 \cdot K_{R_2^s}}{|K_0||K_{R_2^s}|} \right), \quad (4.5)$$

$$\left(\partial_t^2 - c_s^2 \Delta \right) < n_e > = \frac{1}{4\pi m_i} \Delta \left(|E|^2 + \frac{\omega_{pe}^2}{c^2} (|A_0|^2 + |A_{R_1}|^2 + |A_{R_2}|^2 + |A_{R_2^s}|^2) \right). \quad (4.6)$$

Note that since the Raman components are not resonant one another, one gets two distinct equations without coupling terms like $A_{R_1} A_{R_2}^*$ and the same procedure than in Section 2 can be used. A non dimensional form can be obtained. We denote $p = < n_e >$. Using $\frac{1}{\omega_0}$ as time scale, $\frac{1}{|K_0|}$ as space scale and denoting

$$\tilde{A}_0 = \sqrt{\omega_0} \frac{\omega_{pe}}{c} \frac{A_0}{\gamma}, \quad \tilde{A}_{R_1} = \sqrt{\omega_{R_1}} \frac{\omega_{pe}}{c} \frac{A_{R_1}}{\gamma},$$

$$\tilde{A}_{R_2} = \sqrt{\omega_{R_2}} \frac{\omega_{pe}}{c} \frac{A_{R_2}}{\gamma}, \quad \tilde{A}_{R_2^s} = \sqrt{\omega_{R_2^s}} \frac{\omega_{pe}}{c} \frac{A_{R_2^s}}{\gamma},$$

with

$$\gamma = \frac{2m_e\omega_0}{ek_0}\sqrt{\omega_0\omega_{pe}\omega_{R_1}},$$

we obtain (dropping the tildes) and introducing

$$\alpha = \sqrt{\frac{\omega_{R_1}}{\omega_{R_2}}},$$

$$\begin{aligned} i\left(\partial_t + \frac{c^2 k_0^2}{\omega_0^2} \partial_x\right) A_0 + \left(\frac{c^2 k_0^2}{2\omega_0^2} \Delta - \frac{c^4 k_0^4}{2\omega_0^4} \partial_x^2\right) A_0 &= \frac{\omega_{pe}^2}{2\omega_0^2} p A_0 \\ &- \nabla \cdot E \left(A_{R_1} e^{-i\theta_{1,1}} \frac{k_{R_1}}{|K_{R_1}|} + \alpha (A_{R_2} e^{-i\theta_{1,2}} + A_{R_2^s} e^{-i\theta_{1,2s}}) \frac{k_{R_2}}{|K_{R_2}|} \right), \end{aligned} \quad (4.7)$$

$$\begin{aligned} i\left(\partial_t + \frac{c^2 k_0}{\omega_{R_1} \omega_0} K_{R_1} \cdot \nabla\right) A_{R_1} + \frac{1}{2\omega_{R_1} \omega_0} \left(c^2 k_0^2 \Delta - \frac{c^4 k_0^2}{\omega_{R_1}^2} (K_{R_1} \cdot \nabla)^2 \right) A_{R_1} \\ = \frac{\omega_{pe}^2}{2\omega_0 \omega_{R_1}} p A_{R_1} - \nabla \cdot E^* A_0 e^{i\theta_{1,1}} \frac{k_{R_1}}{|K_{R_1}|}, \end{aligned} \quad (4.8)$$

$$\begin{aligned} i\left(\partial_t + \frac{c^2 k_0}{\omega_{R_2} \omega_0} K_{R_2} \cdot \nabla\right) A_{R_2} + \frac{1}{2\omega_{R_2} \omega_0} \left(c^2 k_0^2 \Delta - \frac{c^4 k_0^2}{\omega_{R_2}^2} (K_{R_2} \cdot \nabla)^2 \right) A_{R_2} \\ = \frac{\omega_{pe}^2}{2\omega_0 \omega_{R_2}} p A_{R_2} - \alpha \nabla \cdot E^* A_0 e^{i\theta_{1,2}} \frac{k_{R_2}}{|K_{R_2}|}, \end{aligned} \quad (4.9)$$

$$\begin{aligned} i\left(\partial_t + \frac{c^2 k_0}{\omega_{R_2} \omega_0} K_{R_2^s} \cdot \nabla\right) A_{R_2^s} + \frac{1}{2\omega_{R_2} \omega_0} \left(c^2 k_0^2 \Delta - \frac{c^4 k_0^2}{\omega_{R_2}^2} (K_{R_2^s} \cdot \nabla)^2 \right) A_{R_2^s} \\ = \frac{\omega_{pe}^2}{2\omega_0 \omega_{R_2}} p A_{R_2^s} - \alpha \nabla \cdot E^* A_0 e^{i\theta_{1,2s}} \frac{k_{R_2}}{|K_{R_2}|}, \end{aligned} \quad (4.10)$$

$$\begin{aligned} i\partial_t E + \frac{v_{th}^2 k_0^2}{2\omega_{pe} \omega_0} \Delta E &= \frac{\omega_{pe}}{2\omega_0} p E + \nabla \left(A_0 A_{R_1}^* e^{i\theta_{1,1}} \frac{k_{R_1}}{|K_{R_1}|} \right. \\ &\left. + \alpha (A_0 A_{R_2}^* e^{i\theta_{1,2}} + A_0 A_{R_2^s}^* e^{i\theta_{1,2s}}) \frac{k_{R_2}}{|K_{R_2}|} \right), \end{aligned} \quad (4.11)$$

$$\begin{aligned} \left(\partial_t^2 - c_s^2 \Delta \right) p &= \frac{4m_e}{m_i} \frac{\omega_0 \omega_{R_1}}{\omega_{pe}^2} \Delta \left(|E|^2 + \frac{\omega_{pe}}{\omega_0} |A_0|^2 + \frac{\omega_{pe}}{\omega_{R_1}} |A_{R_1}|^2 \right. \\ &\left. + \frac{\omega_{pe}}{\omega_{R_2}} (|A_{R_2}|^2 + |A_{R_2^s}|^2) \right). \end{aligned} \quad (4.12)$$

Remark 4.1. Note that the only new coefficient is the ratio of the Raman frequencies $\frac{\omega_{R_1}}{\omega_{R_2}}$.

5 Numerical simulations.

5.1 The scheme.

We adapt the scheme introduced in [6]. We consider a regular mesh in space. The fields are approximated by $A_{i,j}$ for $i = 0, \dots, N_x$ and $j = 0, \dots, N_y$. We use periodic boundary conditions that is for all $j = 0, \dots, N_y$, $A_{0,j} = A_{N_x,j}$. In space, we consider centered finite difference discretization for each differential operator. Introducing

$$X_0^{n+1} = \frac{A_0^{n+1} + A_0^n}{2}, \quad X_{R_1}^{n+1} = \frac{A_{R_1}^{n+1} + A_{R_1}^2}{2}, \quad X_{R_2}^{n+1} = \frac{A_{R_2}^{n+1} + A_{R_2}^2}{2},$$

$$X_{R_2^s}^{n+1} = \frac{A_{R_2^s}^{n+1} + A_{R_2^s}^2}{2}, \quad X_E^{n+1} = \frac{E^{n+1} + E^n}{2}, \quad X_p^{n+1} = \frac{p^{n+1} + p^n}{2},$$

as new unknowns, the scheme reads

$$2i \frac{X_0^{n+1} - A_0^n}{\Delta t} + i \frac{c^2 k_0^2}{\omega_0^2} \partial_x X_0^{n+1} + \left(\frac{c^2 k_0^2}{2\omega_0^2} \Delta - \frac{c^4 k_0^4}{2\omega_0^4} \partial_x^2 \right) X_0^{n+1}$$

$$= \frac{\omega_{pe}^2}{2\omega_0^2} X_p^{n+1} X_0^{n+1} - \frac{1}{2} \left(\Psi_E^{n+\frac{1}{2}} X_{R_1}^{n+1} + \nabla \cdot X_E^{N+1} \Phi_{A_{R_1}}^{n+\frac{1}{2}} \right) e^{-i\theta_{1,1}^{N+\frac{1}{2}}} \frac{k_{R_1}}{|K_{R_1}|}$$

$$- \frac{\alpha}{2} \left(\Psi_E^{n+\frac{1}{2}} X_{R_2}^{n+1} + \nabla \cdot X_E^{N+1} \Phi_{A_{R_2}}^{n+\frac{1}{2}} \right) e^{-i\theta_{1,2}^{N+\frac{1}{2}}} \frac{k_{R_2}}{|K_{R_2}|}$$

$$- \frac{\alpha}{2} \left(\Psi_E^{n+\frac{1}{2}} X_{R_2^s}^{n+1} + \nabla \cdot X_E^{N+1} \Phi_{A_{R_2^s}}^{n+\frac{1}{2}} \right) e^{-i\theta_{1,2^s}^{N+\frac{1}{2}}} \frac{k_{R_2}}{|K_{R_2}|}, \quad (5.1)$$

where

$$\frac{\Psi_E^{n+\frac{1}{2}} + \Psi_E^{n-\frac{1}{2}}}{2} = \nabla \cdot E^n, \quad \frac{\Phi_{A_{R_1}}^{n+\frac{1}{2}} + \Phi_{A_{R_1}}^{n-\frac{1}{2}}}{2} = A_{R_1}^n,$$

$$\frac{\Phi_{A_{R_2}}^{n+\frac{1}{2}} + \Phi_{A_{R_1}}^{n-\frac{1}{2}}}{2} = A_{R_1}^n, \quad \frac{\Phi_{A_{R_2^s}}^{n+\frac{1}{2}} + \Phi_{A_{R_2^s}}^{n-\frac{1}{2}}}{2} = A_{R_2^s}^n,$$

are auxiliary functions. The equations of System (4.8) – (4.12) are discretized in the following way

$$2i \frac{X_{A_{R_1}}^{n+1} - A_{R_1}^n}{\Delta t} + \frac{c^2 k_0}{\omega_{R_1} \omega_0} K_{R_1} \cdot \nabla X_{R_1}^{n+1} + \frac{1}{2\omega_{R_1} \omega_0} \left(c^2 k_0^2 \Delta - \frac{c^4 k_0^2}{\omega_{R_1}^2} (K_{R_1} \cdot \nabla)^2 \right) X_{R_1}^{n+1}$$

$$= \frac{\omega_{pe}^2}{2\omega_0 \omega_{R_1}} X_p^{n+1} X_{R_1}^{n+1} - \left(\Psi_E^{n+\frac{1}{2}} \right)^* X_0^{n+1} e^{i\theta_{1,1}^{n+\frac{1}{2}}} \frac{k_{R_1}}{|K_{R_1}|}, \quad (5.2)$$

$$2i \frac{X_{A_{R_2}}^{n+1} - A_{R_2}^n}{\Delta t} + \frac{c^2 k_0}{\omega_{R_2} \omega_0} K_{R_2} \cdot \nabla X_{R_2}^{n+1} + \frac{1}{2\omega_{R_2} \omega_0} \left(c^2 k_0^2 \Delta - \frac{c^4 k_0^2}{\omega_{R_2}^2} (K_{R_2} \cdot \nabla)^2 \right) X_{R_2}^{n+1}$$

$$= \frac{\omega_{pe}^2}{2\omega_0 \omega_{R_2}} X_p^{n+1} X_{R_2}^{n+1} - \left(\Psi_E^{n+\frac{1}{2}} \right)^* X_0^{n+1} e^{i\theta_{1,2}^{n+\frac{1}{2}}} \frac{k_{R_2}}{|K_{R_2}|}, \quad (5.3)$$

$$\begin{aligned}
& 2i \frac{X_{A_{R_2^s}}^{n+1} - A_{R_2^s}^n}{\Delta t} + \frac{c^2 k_0}{\omega_{R_2} \omega_0} K_{R_2^s} \cdot \nabla X_{R_2^s}^{n+1} + \frac{1}{2\omega_{R_2} \omega_0} \left(c^2 k_0^2 \Delta - \frac{c^4 k_0^2}{\omega_{R_2}^2} (K_{R_2} \cdot \nabla)^2 \right) X_{R_2^s}^{n+1} \\
& = \frac{\omega_{pe}^2}{2\omega_0 \omega_{R_2}} X_p^{n+1} X_{R_2^s}^{n+1} - \left(\Psi_E^{n+\frac{1}{2}} \right)^* X_0^{n+1} e^{i\theta_{1,2s}^{n+\frac{1}{2}}} \frac{k_{R_2}}{|K_{R_2}|}, \tag{5.4}
\end{aligned}$$

$$\begin{aligned}
& i \frac{X_E^{n+1} - X_E^n}{\Delta t} + \frac{v_{th}^2 k_0^2}{2\omega_{pe} \omega_0} \Delta X_E^{n+1} = \frac{\omega_{pe}}{2\omega_0} X_p^{n+1} X_E^{n+1} + \nabla \left(X_0^{n+1} \left(\Phi_{A_{R_1}}^{n+\frac{1}{2}} \right)^* e^{i\theta_{1,1}^{n+\frac{1}{2}}} \frac{k_{R_1}}{|K_{R_1}|} \right. \\
& \left. + \alpha \left(X_0^{n+1} \left(\Phi_{A_{R_2}}^{n+\frac{1}{2}} \right)^* e^{i\theta_{1,2}^{n+\frac{1}{2}}} + X_0^{n+1} \left(\Phi_{A_{R_2^s}}^{n+\frac{1}{2}} \right)^* e^{i\theta_{1,2s}^{n+\frac{1}{2}}} \right) \frac{k_{R_2}}{|K_{R_2}|} \right), \tag{5.5}
\end{aligned}$$

$$\begin{aligned}
& \frac{p^{n+1} - 2p^n + p^{n-1}}{\Delta t^2} - c_s^2 \Delta \left(\frac{p^{n+1} + p^{n-1}}{2} \right) = \frac{4m_e}{m_i} \frac{\omega_0 \omega_{R_1}}{\omega_{pe}^2} \Delta \left(|E^n|^2 + \frac{\omega_{pe}}{\omega_0} |A_0^n|^2 \right. \\
& \left. + \frac{\omega_{pe}}{\omega_{R_1}} |A_{R_1}^n|^2 + \frac{\omega_{pe}}{\omega_{R_2}} (|A_{R_2}^n|^2 + |A_{R_2^s}^n|^2) \right). \tag{5.6}
\end{aligned}$$

The scheme is inspired from that of C. Besse [3] and B. Glassey [7].

5.2 The test case.

The values of the different parameters are the same than the ones used in [6] and we refer to [6] for a complete description. In particular, v_0 , v_{R_1} and v_{R_2} denotes respectively the propagation speed of A_0 , A_{R_1} and A_{R_2} . We denote θ the angle between the wave vectors of A_0 and A_{R_2} and by θ_{\max} the angle corresponding to the maximum amplification rate for the Raman component propagating in the forward direction. We work on a system in dimensionless form. The unit of lenght is $\frac{1}{k_0}$ and the unit in time is $\frac{1}{\omega_0}$. The spatial domain is $x \in [0, 300]$ and $y \in [0, 200]$. The number of discretization points in x is $N_x = 300$ and the one in y is $N_y = 200$. We compute on a time intervall $[0, T]$ with $T = 200$. The number of time steps is $N_t = 576$. The initial data for A_0 is of the form

$$A_0(0, \cdot) = \alpha e^{-\beta_x(x-\gamma_x)^2} e^{-\beta_y(y-\gamma_y)^2}.$$

• **Case 1:** We consider a collision test case. We take $\theta = \theta_{\max}$. We define $\alpha = 0.1$, $\beta_x = \frac{1}{1250}$, $\beta_y = \frac{1}{1800}$. The collision takes place at the point $x = 100$, $y = 100$. Taking into account the propagation speed of the different fields, we introduce the following parameters

$$L_{R_1}^x = \frac{v_{R_1}}{v_0} * 50, \quad L_{R_2}^x = \frac{v_{R_2}}{v_0} * 50 * \cos(\theta), \quad L_{R_2}^y = 100 - L_{R_2}^x * \tan(\theta).$$

We take

$$\begin{cases} A_0(0, \cdot) = \alpha e^{-\beta_x(x-50)^2} e^{-\beta_y(y-100)^2}, \\ A_R^1 = \frac{\alpha}{100} e^{-\beta_x(x-(100+L_{R_1}^x))^2} e^{-\beta_y(y-100)^2}, \\ A_R^2 = \frac{\alpha}{100} e^{-\beta_x(x-(100-L_{R_2}^x))^2} e^{-\beta_y(y-L_{R_2}^y)^2}. \end{cases} \tag{5.7}$$

This case corresponds to the maximum amplification rate for the second Raman component that is $\theta = \theta_{\max}$.

- **Case 2:** We now let θ varying from $\frac{1}{6}\theta_{\max}$ to $\frac{4}{3}\theta_{\max}$ and we keep $L_{R_2}^y = 100 - L_{R_2}^x * \tan(\theta)$. The initial conditions are the same than the ones used for case 1.

5.3 Comments

For convenience we have rescaled all the fields. For each component, the maximum of the modulus is equal to 100. In Figure 4, we can observe the very begining of the interaction at time $t = 50$. The maximum of the amplitude of A_0 is still near its maximum whereas the ones for A_{R_1} and A_{R_2} are far from their maximum. In Figure 5, we have reached the impact point. The support of the different Gaussians are nearly equal and so the amplification process is maximal. The two Raman components are growing exponentially whereas the amplitude of the incident laser field is decreasing. It is of course in agreement with the conservation law coming from System (4.7) – (4.12) and preserved by our numerical scheme

$$\frac{d}{dt} \int_{\mathbb{R}^n} \left(2|A_0|^2 + |A_{R_1}|^2 + |A_{R_2}|^2 + |A_{R_2}^s|^2 + |E|^2 \right) ds = 0.$$

In Figure 6, the interaction has stopped since the supports became disjoints. One can observe the effects of the dispersion on the fields.

In Figure 7, we have ploted the maximum of the fields A_{R_1} and A_{R_2} with respect to the parameter $\gamma = \frac{\theta}{\theta_{\max}}$. We can observe that the angle θ has no influence of the fields A_{R_1} . The influence on A_{R_2} is of great interest. As expected, the maximum for A_{R_2} is achieved for $\gamma = 1$. Furthermore one can observe that the process is much more efficient for $\gamma = 1$ than for example $\gamma = \frac{1}{6}$. Indeed, the ratio between the two maximum of the amplitude is around 20 per cent, which means that the gain is considerable.

Note that the shapes of the curves of Figure 3 and Figure 7 are not the same although the maximum is reached at the same point. It is due to the fact that Figure 3 comes from a very basic analysis while Figure 7 takes into account all the complex phenomenas involved in the Raman instability. For example the influence of the fluctuation of the density of ions is crucial and it is not taken into account in the linear analysis developped in Section 3.2. However we would like to emphasize that we obtain the right angle leading to the maximum amplification rate. Moreover, the curve of Figure 7 is flat at the maximum. It is due to the fact that the pulse is not monochromatic and therefore even if we prescribe the angle at a value that is different from the one giving the maximum amplification rate, a larger region is involved. Geometrically and finally, the critical value is also concerned and the amplification is larger than that predicted by the linear theory.

References

- [1] R. Belaouar, T. Colin, G. Gallice and C. Galusinski. *Theoretical and numerical study of a quasilinear system describing Landau damping.* M2AN Math. Model. Numer. Anal., Vol. 40(6), (2006), 961-990.
- [2] T.B. Benjamin, J.L. Bona and J.J. Mahony. *Model equations for long waves in nonlinear dispersive systems.* Philos. Trans. Roy. Soc. London Ser. A, Vol. 272(1220), (1972), 47-78
- [3] C. Besse. *Schéma de relaxation pour l'équation de Schrödinger non linéaire et les systèmes de Davey et Stewartson.* C.R. Acad. Sci. Paris. Sér. I Math., Vol. 326, (1998), 1427-1432.
- [4] J. Bona, H. Chen, S.M. Sun, B.-Y. Zhang, *Comparison of quarter-plane and two-point boundary value problems: the BBM-equation.* Discrete Contin. Dyn. Syst. 13 (2005), no. 4, 921–940.
- [5] M. Colin and T. Colin. *On a quasi-linear Zakharov system describing laser-plasma interactions.* Diff. Int. Eqs, Vol. 17, 3-4, (2004), 297-330.
- [6] M. Colin and T. Colin. *A numerical model for the Raman amplification for laser-plasma interactions.* J. Comput. App. Math., Vol. **193**, 2, (2006), 535-562.
- [7] R.T. Glassey. *Convergence of an energy-preserving scheme for the Zakharov equation in one space dimension.* Math. of Comput. Vol. 58, Number 197, (1992), 83-102.

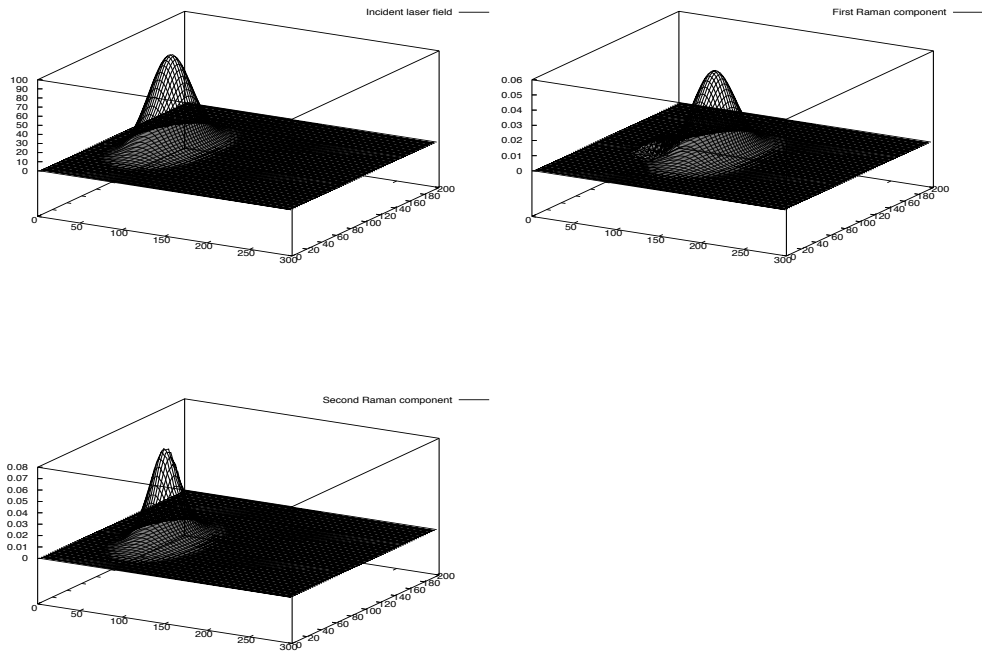


Figure 4: 2D-geometry. Modulus of the rescaled fields at time $t=50$ with initial conditions (5.7). From left to right, first line A_0 and A_{R_1} , second line A_{R_2} .

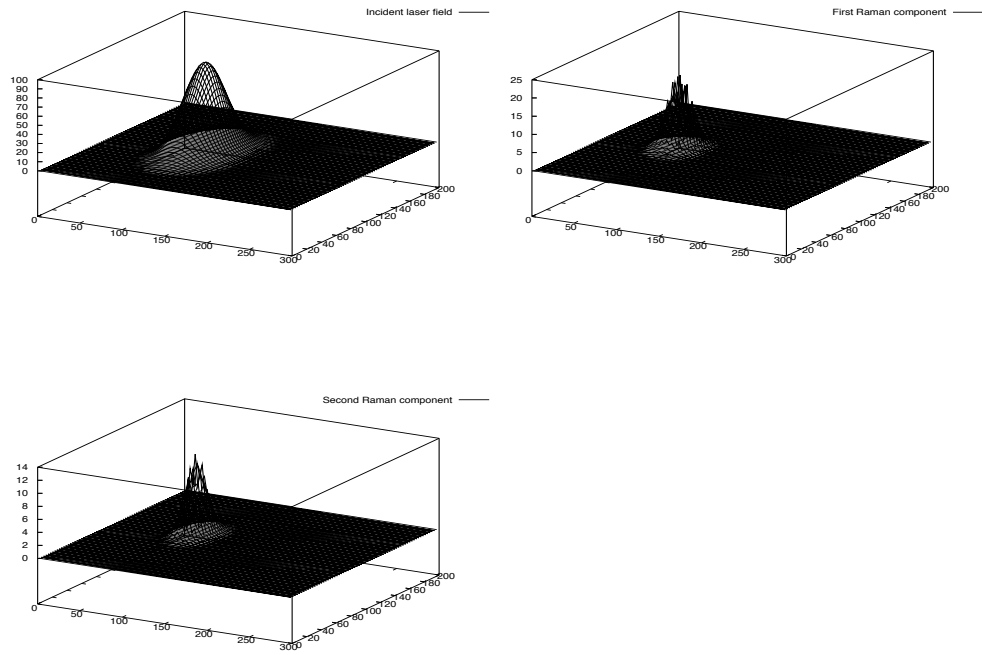


Figure 5: 2D-geometry. Modulus of the rescaled fields at time $t=66$ with initial conditions (5.7). From left to right, first line A_0 and A_{R_1} , second line A_{R_2} .

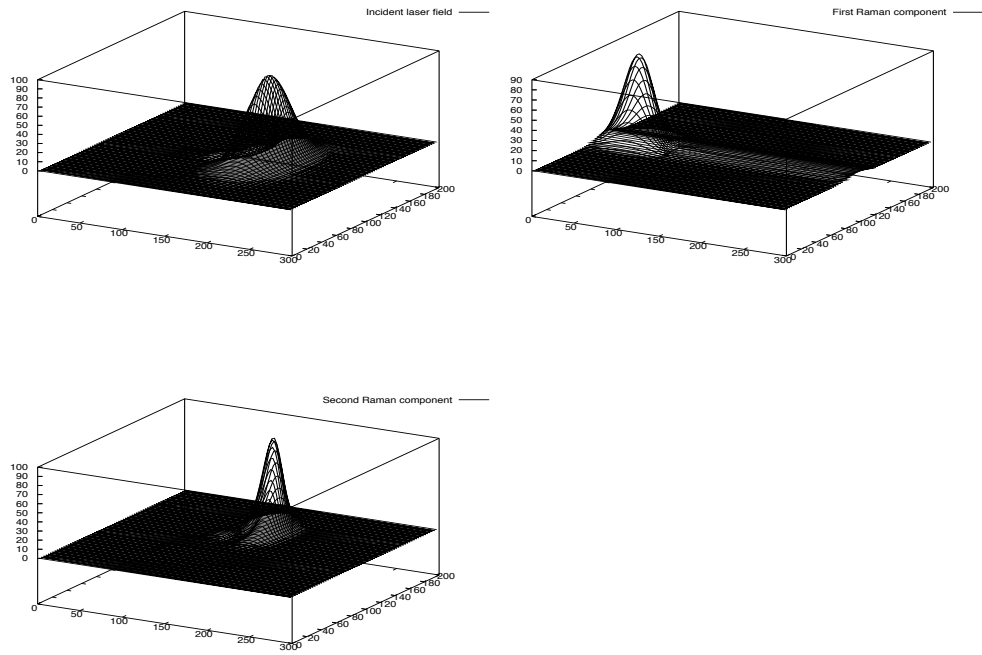


Figure 6: 2D-geometry. Modulus of the rescaled fields at time $t=150$ with initial conditions (5.7). From left to right, first line A_0 and A_{R_1} , second line A_{R_2} .

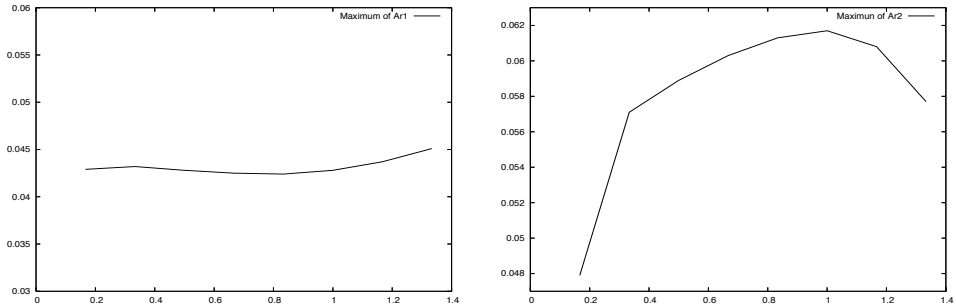


Figure 7: Maximum of the fields with respect to the parameter $\gamma = \frac{\theta}{\theta_{\max}}$. We let gamma vary from $\frac{1}{6}$ to $\frac{8}{6}$. From left to right, A_{R_1} and A_{R_2} .